A large ^{14}C excursion in 5480 BC indicates an abnormal sun in the Mid Holocene

Fusa Miyake[1], A. J. Timothy Jull[2,3], Irina P. Panyushkina[4], Lukas Wacker[5], Matthew Salzer[4], Chris Baisan[4], Todd E. Lange[3], Richard Cruz[3], Kimiaki Masuda[1], Toshio Nakamura[1]

Authors information

Name	Current postal	e-mail address
Fusa Miyake	1	fmiyake@isee.nagoya-u.ac.jp
A. J. Timothy Jull	2,3	jull@email.arizona.edu
Irina P. Panyushkina	4	ipanyush@email.arizona.edu
Lukas Wacker	5	wacker@phys.ethz.ch
Matthew Salzer	4	msalzer@ltrr.arizona.edu
Chris Baisan	4	cbaisan@ltrr.arizona.edu
Todd E. Lange	3	lange@physics.arizona.edu
Richard Cruz	3	cruz@physics.arizona.edu
Kimiaki Masuda	1	kmasuda@isee.nagoya-u.ac.jp
Toshio Nakamura	1	nakamura@nendai.nagoya-u.ac.jp

[1]Institute for Space-Earth Environmental Research, Nagoya University, Chikusa-ku, Nagoya 464-8601, Japan

[2]Department of Geosciences, University of Arizona, Tucson, AZ 85721 USA

[3]University of Arizona AMS laboratory, Physics Building, Tucson, AZ 85721 USA

[4]Laboratory of Tree Ring Research, University of Arizona, Tucson, AZ 85721 USA

[5]AMS laboratory, ETH Hönggerberg, CH-8092 Zürich, Switzerland

Radiocarbon content in tree-rings can be an excellent proxy of the past incoming cosmic ray intensities to the Earth. Although such past cosmic ray variations have been studied by measurements of ^{14}C contents in tree rings with ≧10 year time resolution for the Holocene (1), there are few annual ^{14}C data. There is a little understanding about annual ^{14}C variations in the past with the exception of a few periods including the AD774-775 annual ^{14}C excursion (2).

Here, we report the result of ^{14}C measurements using the bristlecone pine tree rings for the period from 5490 BC to 5411 BC with 1-2 year resolution, and a finding of an extraordinarily large ^{14}C increase (20‰) from 5481 BC to 5471 BC (the 5480 BC event). The ^{14}C increase rate of this event is much larger than that of the normal Grand Solar Minima. We propose the possible causes of this event are a special phase of grand solar minimum, or a combination of successive solar proton events and a normal grand solar minimum (or solar magnetic activity).

Introduction

Cosmic rays reaching the Earth are generally classified as a Galactic Cosmic Rays (GCR) and a Solar Cosmic Rays (SCR). GCR including protons, heavier nuclei, electrons, gamma-ray, etc. originate from outside the heliosphere and its intensity to the Earth is modulated by the interplanetary magnetic field. SCR, which can also result from episodic Solar Proton Events (SPE) originate from particle acceleration in the solar corona. Incoming cosmic rays interact with the atmosphere and generate an atmospheric cascade, which produces various types of particle components (3). Since cosmogenic nuclides such as ^{14}C and ^{10}Be are produced in an atmospheric cascade process, their concentrations show the cosmic ray intensities.

The ^{14}C contents in tree rings are normally varied by the solar magnetic activities and the geomagnetic activities, which modulate the GCR flux to the Earth (4). There is an excellent tree-ring record of ^{14}C data in the international radiocarbon calibration curve IntCal (1). This record has a typically 10 year resolution extending to 13,900BP. We can see solar- and geo-magnetic variations exhibited in the radiocarbon record as decadal to millennial time scale, i.e. 50-100 years variation such as grand solar minima, and ~1000 years variations of the geomagnetic dipole moment (5).

On the other hand, there is little understanding of annual ^{14}C variations due to the lack of annual ^{14}C data for periods before AD 1510 (6). Previously, it has been considered that annual variations of ^{14}C contents do not change rapidly because original signals are diluted and attenuated by the carbon cycle (5). Although most of

annual ^{14}C data show a gradual variation, those in some periods show significant and rapid annual changes. The AD 775 and AD 994 (or AD 993) events are two examples of large changes which occur at annual resolution (2,7). The ^{14}C variation of these two events have a characteristic increase over 1-2 years followed by a decay which reflects a rapid input of cosmic rays to the atmosphere within 1-year and the decay by the global carbon cycle. The most likely explanation of these events is that they were the result of extreme Solar Proton Events (SPEs), based on verifications of annual ^{14}C measurements using worldwide tree samples (8-11) and annual ^{10}Be measurements in ice cores from the Antarctica and the Greenland (12-14). It is possible that there are more annual cosmic ray events like the 775 event and even other types of annual rapid ^{14}C variation in the past.

In order to find more rapid changes in ^{14}C data at annual resolution, we have surveyed the periods where ^{14}C increase rates are large in the IntCal (1) record. If such annual changes had occurred in the past, it is possible that such events would be manifest in the IntCal data, since a large change in 1-2 years would be observed in the averaged 5-10 years data. As a result, there are 15 intervals where increase rates are $\geqq$0.3 [‰/year] (using min-max values) in the IntCal13 data (1) for the Holocene (last 12,000 years) (15). The 5460 BC peak from 5490 BC to 5460 BC has one of the largest increase rates (0.51[‰/year]) in the Holocene. We selected the period for our annual measurement for interval 5490-5411 BC in order to investigate the structure of the ^{14}C signal around 5460 BC.

Method and Result

We used a bristlecone pine specimen from the White Mountains (California, US) for annual ^{14}C measurements. Further information about the wood is described in the supplementary information (figure S1). We prepared the cellulose samples by a standard chemical cleaning methods at the AMS (Accelerator Mass Spectrometry) laboratory in the University of Arizona, and measured ^{14}C contents at three different AMSs (University of Arizona, Nagoya University, and Swiss Federal Institute of Technology: ETH) to cross-validate our results and ascertain any laboratory offset between different AMS system.

Figure 1 (upper) shows ^{14}C results of 3 replicated series from our measurements. Since the 3 series are consistent with each other, we can immediately conclude that there is no laboratory offsets between the different AMS measurements. Since the values for the same year all agree within 2-sigma (95% probability), we combined 3 series shown in the figure 1 (upper). Figure 1 (lower)

shows a comparison between the combined data and the IntCal13 (1). The combined data are almost consistent with the IntCal13 and original data of the IntCal13.

From our measurements, it becomes clear that the marked increase in the IntCal13 data (5490-5460 BC) shows a very large change in annual resolution. The increase occurred from 5481 BC to 5473 BC (or 5485-5471 BC: min-max values), and the increase rates are 17.0‰/8years (or 26.2‰/14years), respectively. Although a variation of this event (hereafter we call the event as the 5480 BC event) is different from the previously-identified events like the AD 775 event, the total increase in ^{14}C contents of the event is larger than that of the AD 775 event (~15‰). We show a comparison between the 5480 BC event and the AD 775 event in figure S2.

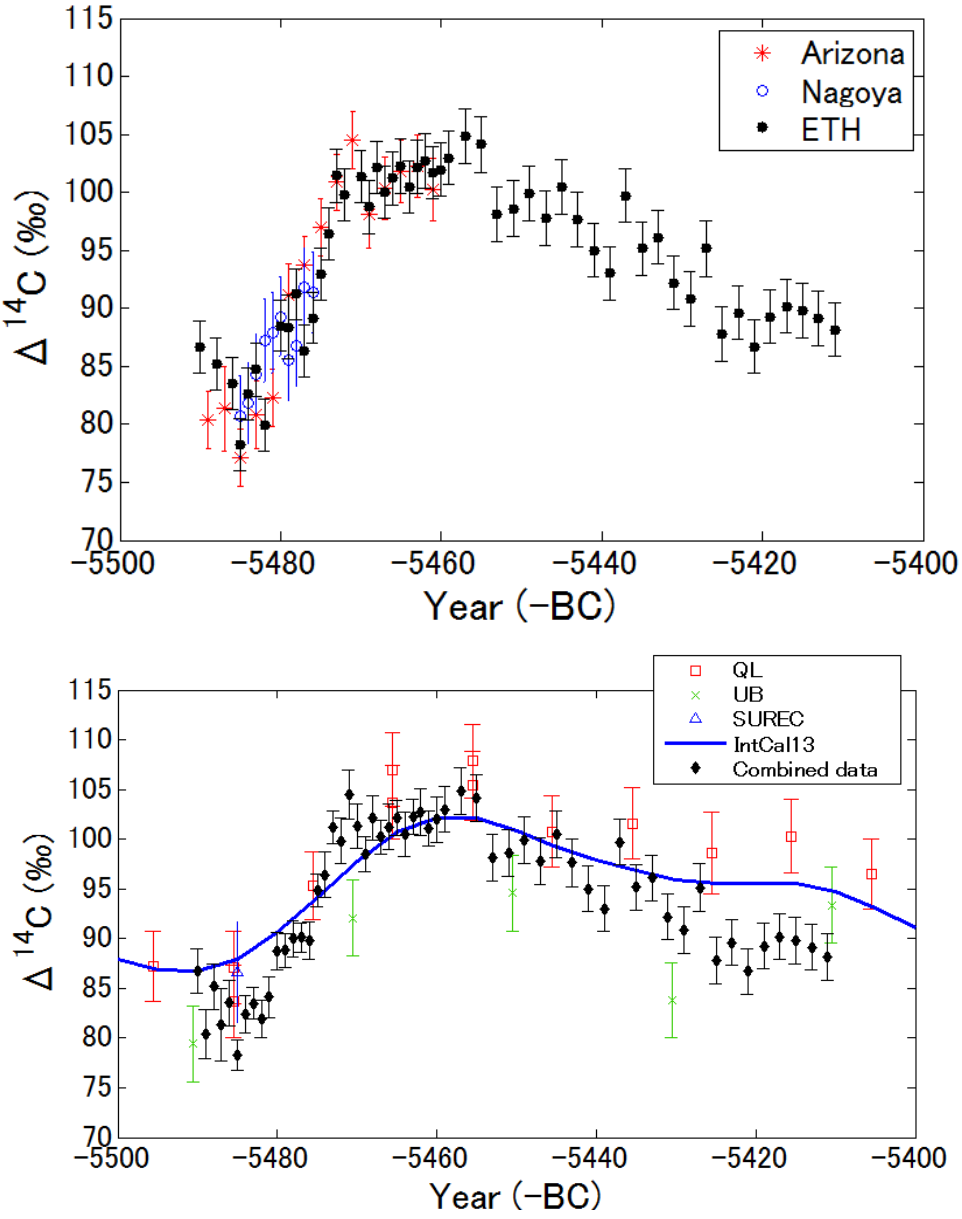

Figure 1: (upper) Measured results ($\Delta^{14}C$: defined in Stuiver & Polach [1977] (30)) of 3 series which were measured at different AMSs (Arizona, Nagoya, and ETH). (lower) Comparison of our combined data (diamonds: bristlecone pine), the original datasets of the IntCal (QL (6), UB (31), and SUREC (32)), and the IntCal13 curve (1). Although the IntCal original data are not consistent with each other, our measured results almost agree with the IntCal13.

Discussion

Previous studies classified the peak around 5460 BC as a grand solar minimum using the IntCal data (16-18). Grand solar minima are defined as the periods when the solar activity is at very low level, i.e. it is defined as group sunspot number becomes less than 15 during at least two consecutive decades according to Usoskin et al. (18). In a grand solar minimum, the ^{14}C content increases largely due to a reduction of the solar modulation parameter Φ (it is estimated that Φ was ~160 [MV] during the Maunder Minimum, while the present-day value varies between 400-1000 [MV] (19)).

We compared the annual 5480 BC event with other grand solar minima, that is the Maunder, the Spörer, the Oort, the AD7th century and the 4th century BC grand solar minima, where we have annual resolution ^{14}C data (6, 20-22). Figure 2 shows a comparison between our combined datasets and other grand solar minima. The origin of the coordinates corresponds to the shifted data point of the first year of each grand solar minima (18), and the 5481 BC data point. An average of the increase rate of the other five grand solar minima is about 0.3‰/year (more details on the grand solar minima are provided in the supplementary information). Against the normal grand solar minima, the increase rate of the 5480 BC event is 2‰/year. Although the total ^{14}C increment of the 5480 BC event is almost equal to the other minima (~20‰), the 5480 BC event increases much faster than the others. Therefore, we expect that the origin of the 5480 BC event is apparently different from the other normal grand solar minima.

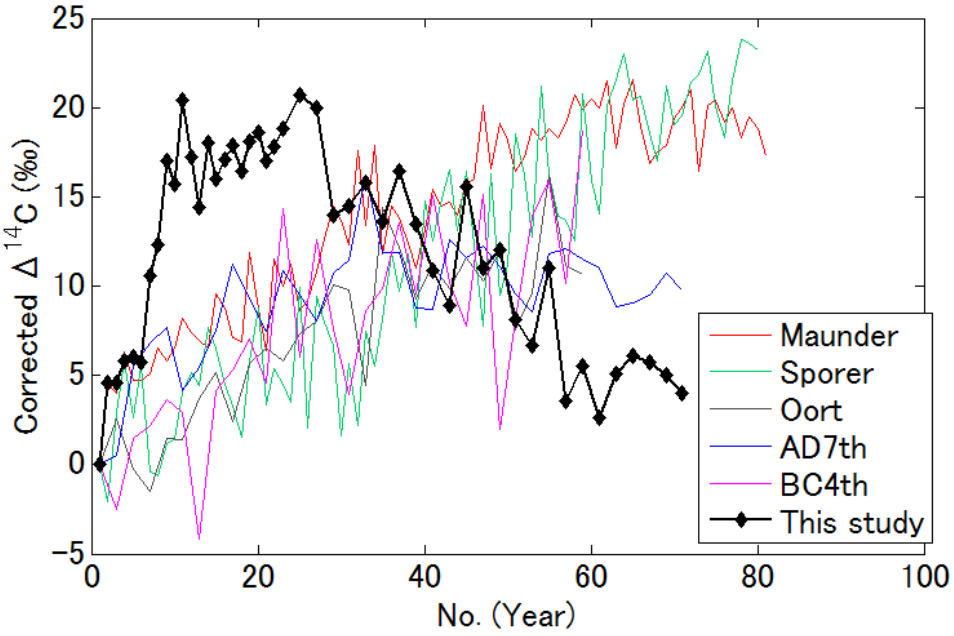

Figure 2: Comparison of the 5480 BC event between the present data and other grand solar minima (6, 20-22). Further information about the grand solar minima is provided in the supplementary information (table S1).

We hypothesize that plausible causes of this 5480 BC event are 1) special state of the grand solar minimum, 2) successive extreme SPEs over ~20 years, and 3) combination of some extreme SPEs and a normal grand solar minimum (or solar magnetic activities). Apart from these causes, changes in the geomagnetic field can also affect the GCR flux to the Earth. But it is generally considered that the geomagnetic field does not change over several centuries (5). Although the geomagnetic dipole field was ~0.9 times smaller than today's field, almost constant value continued over ~3000 years from ca. 6000 BC to 3000 BC (23). Therefore we do not consider the effect of the geomagnetic effect. Also a change of the oceanic carbon cycle and reservoir age would affect ^{14}C, however ocean-circulation events cannot explain ^{14}C variations on a decadal scale, these normally require up to 200 years, as shown in a study of the Younger Dryas event by Singarayer et al. (24). Although another galactic event, e.g. GCR flux increases ~10 years followed by a tail (a few decades) may explain the 5480 BC event, we don't know such event with our present knowledge.

First, we consider the case of special state of the grand solar minimum. We

calculated a production rate for our measured periods using a 4-box carbon cycle model (figure S4). We assumed that the start point (5484 BC) was at steady state pre-industrial value 1.8 [atoms/cm^2/sec] (14). Figure 3 shows this calculated ^{14}C production rate in comparison with the Δ^{14}C data. Note that the steady state value is an assumption, and we cannot conduct a sufficient reconstruction such as the Holocene continuous reconstruction of the decadal ^{14}C production (25) for annual production rates, because we only have restricted data. Hence, we cannot say if our calculated production rates are absolutely correct or not. However, this is the only approach to calculate the annual production rates, and our calculation for a production rate of the 775 event is consistent with other studies (11). Since the geomagnetic field around 5480 BC is 0.9 times smaller than the present value, the steady state of the ^{14}C production rate is supposed as 1.1 times larger than the pre-industrial value (~2.0 [atoms/cm^2/sec]). Then the production rate in the figure 3 should add 0.2 [atoms/cm^2/sec]. However, in order to compare with other ^{14}C production data of different time age (following discussions), we use 1.8 [atoms/cm^2/sec] for convenience.

According to several studies, if the solar modulation parameter becomes zero, the ^{14}C production rate can increase to 3.0 [atoms/cm^2/sec] (19, 26, 27). Averages of the production data for the periods of 5476-71 BC (6 years), 5482-71 BC (10 years) and 5482-57 BC (25 years) are 2.9, 2.6 and 2.35 [atoms/cm^2/sec], respectively. From these, if the 5480 BC event was caused only by solar magnetic activity, the solar modulation parameter must be almost zero for approximately 5 years. The production data for 5481-80 BC, 5476-75 BC, 5474-73 BC, 5472-71 BC, and 5469-68 BC are over 3.0 [atoms/cm^2/sec] (but within 3.0 considering the error), and it may be difficult to explain these data by the solar magnetic variation because the modulation parameter becomes almost zero, however we cannot fully exclude a very weak sun.

The variation after the rapid increase (after 5470 BC) shows a gradual increase (almost a plateau) for 15 years and then shows a gradual decay. Although the increase in ^{14}C for this event is different from the behavior in a normal grand solar minima, the time scale of the plateau and the following decay is consistent with the Maunder Minimum (see figure S6). Here, we have assumed the Maunder Minimum is a standard variation of a grand solar minimum. Therefore, if our event is explained only by a grand solar minimum, this means the solar activity rapidly decreased to an extremely low level, and then, the solar activity became gradually higher, in a similar way to other grand solar minima.

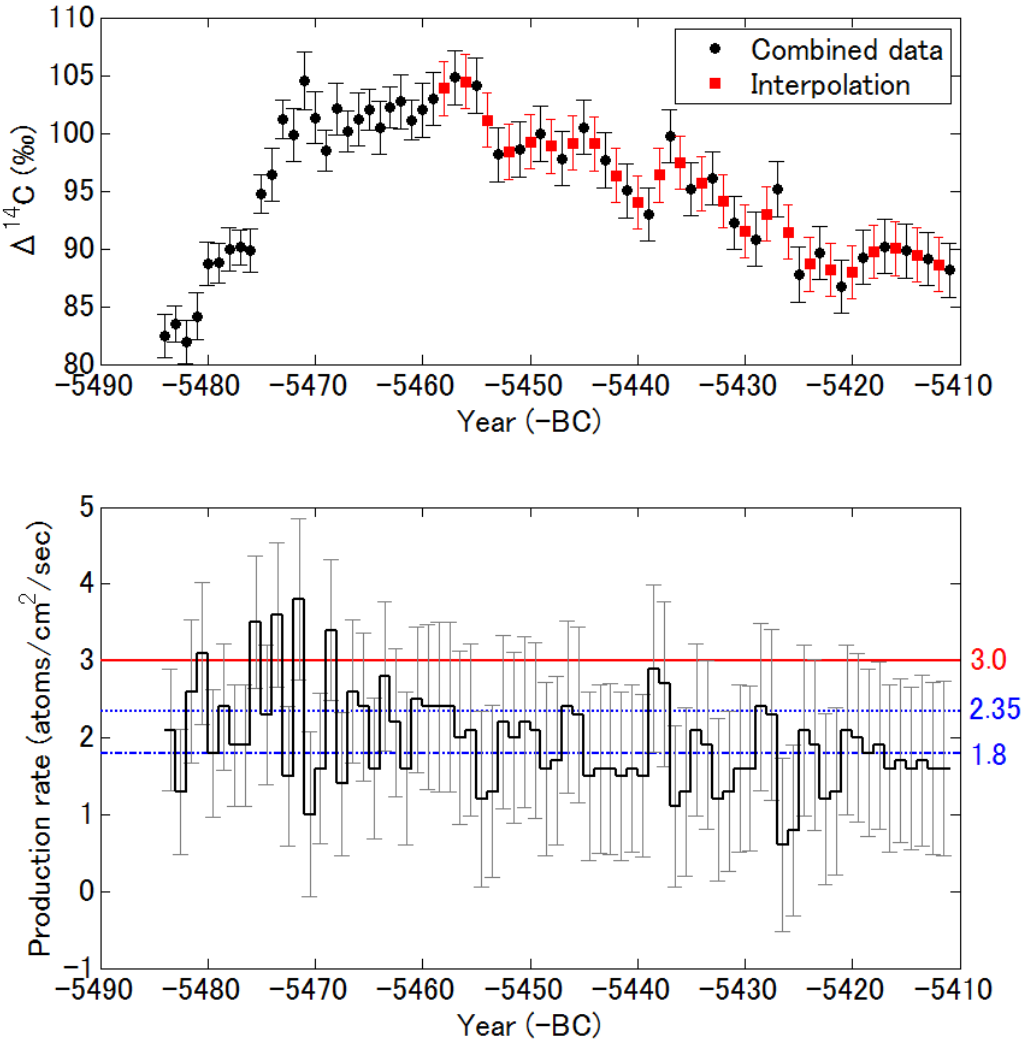

Figure3: ^{14}C production rate for the period from 5484 BC to 5411 BC using 4-box model. We calculated the production rates in this graph using the steady state as 1.8 [atoms/cm^2/sec] (note that the steady state around 5480 BC should be ~2 [atoms/cm^2/sec], so more reliable production rates are +0.2 to the values in this graph). The blue dashed line (1.8 [atoms/cm^2/sec]) marks the production rate of normal solar magnetic activity, the blue dotted line (2.35 [atoms/cm^2/sec]) is average production rate for the Maunder Minimum, and the red solid line (3.0 [atoms/cm^2/sec]) is the production rate in the case the solar modulation parameter becomes zero.

Second, we consider the cases of successive SPEs and the combination of SPEs and a solar magnetic activity. Although it is in principal possible that the variation is explained only by solar energetic particles over the whole period, it is not possible to explain the plateau and the following decay only by SPEs.

Since it is difficult to divide ^{14}C variations into contribution by solar magnetic activities and that by SPEs, we suggest the following two scenarios: I) several SPEs occurred during the early-normal grand solar minimum, or II) several SPEs occurred, and then, the solar magnetic activity became gradually higher. Here, we assume SPEs only occurred in the increasing period (5481-5468 BC: this interval contains the data where production rates >3.0 [atoms/cm^2/sec]). Since we know that a ^{14}C production rate during the Maunder Minimum varies between 2.1 and 2.6 [atoms/cm^2/sec] (19), we can assume a production rate by the low solar magnetic activity during the increasing ^{14}C period is an average of upper values, 2.35 [atoms/cm^2/sec]. In contrast, we note that the production rate of normal solar magnetic activity is 1.8 [atoms/cm^2/sec]. Based on these hypotheses, a total ^{14}C production by SPEs above 2.35 [atoms/cm^2/sec] and 1.8 [atoms/cm^2/sec] during the increase can be shown to be 6.0 [atoms/cm^2/sec] and 10.5 [atoms/cm^2/sec], respectively. The total production rate of the AD 775 event has been estimated to be 3.9-6.9 [atoms/cm^2/sec] (8, 10, 11, 14). Then, in the case of scenario I, ^{14}C production is dominated by the very low modulation parameter and the total production by SPEs is comparable to that of the AD 775 event. In the case of scenario II, the total SPE production must be larger than the AD 775 event.

From direct measurements of the sun, we know solar flares tend to occur during a solar maximum, e.g. the number of SPEs increase in solar maximum periods (28). Also, the two annual ^{14}C events (AD 774-775 and AD 993-994) occurred in higher solar activity periods, or at least did not occur during grand solar minimum periods (7). Thus, we suggest that scenario I (several SPEs occurred in the grand solar minimum) is unlikely, however we cannot exclude scenario I because the mechanism of an occurrence of extreme SPEs is not yet fully understood.

In the observation of solar-type stars by the Kepler telescope, stars which occurred several super-flares for several years were detected (29). Such observations of solar-type stars may support an extreme SPE origin of the 5480 BC event. Further investigations of the ^{14}C record may turn up similar events, which can then compare to events observed in astronomical data.

In any case, ^{14}C variation of the 5480 BC event is extraordinary in the Holocene,

and this event indicates the abnormal solar activity compared to other periods.

References

1. Reimer PJ, et al. (2013) IntCal13 and Marine13 radiocarbon age calibration curves, 0–50,000 years cal BP. Radiocarbon 55(4): 1869–87.
2. Miyake F, Nagaya K, Masuda K, Nakamura T. (2012) A signature of cosmic-ray increase in AD 774–775 from tree rings in Japan. Nature 486: 240–242.
3. Burr GS (2013) Radiocarbon dating: Causes of temporal variations. In "Encyclopedia of Quaternary Science" (eds. S. Elias and C. J. Mock) Amsterdam: Elsevier, pp. 336-344.
4. van der Plicht (2013) J. Radiocarbon Dating: Variations in atmospheric ^{14}C" In "Encyclopedia of Quaternary Science" (eds. S. Elias and C. J. Mock) Amsterdam: Elsevier, pp. 329-335.
5. Beer J, McCracken K, Steiger R (2012) Cosmogenic Radionuclide Theory in the Terrestrial and Space Environments, Springer, Berlin.
6. Stuiver M, Reimer PJ, Braziunas TF (1998) High-precision radiocarbon age calibration for terrestrial and marine samples. Radiocarbon 40: 1127-1151.
7. Miyake F, Masuda K, Nakamura T (2013) Another rapid event in the carbon-14 content of tree rings. Nat. Commun. 4:1748, doi: 10.1038/ncomms2783.
8. Usoskin IG, et al. (2013) The AD775 cosmic event revisited: the Sun is to blame. Astronomy & Astrophysics 552: L3, doi:10.1051/0004-6361/201321080.
9. Jull AJT, et al. (2014) Excursions in the ^{14}C record at A.D. 774–775 in tree rings from Russia and America. Geophys. Res. Lett. 41(8): 3004–3010.
10. Güttler D, et al. (2015) Rapid increase in cosmogenic ^{14}C in AD 775 measured in New Zealand kauri trees indicates short-lived increase in ^{14}C production spanning both hemispheres. Earth and Planetary Science Letters 411: 290–297.
11. Miyake F, et al. (2014) Verification of the cosmic-ray event in AD 993-994 by using a Japanese Hinoki tree. Radiocarbon 56(4): 1–6.
12. Miyake F, et al. (2015) Cosmic ray event of A.D. 774–775 shown in quasi-annual ^{10}Be data from the Antarctic Dome Fuji ice core. Geophys. Res. Lett. 42: 84-89.
13. Sigl M, et al. (2015) Timing and climate forcing of volcanic eruptions for the past 2,500 years. Nature 523: 543-549.
14. Mekhaldi F, et al. (2015) Multiradionuclide evidence for the solar origin of the cosmic-ray events of AD 774/5 and 993/4. Nat. Commun. 6:8611, doi:10.1038/ncomms9611.
15. Miyake F, et al. (2016) Search for annual carbon-14 excursions in the past,

Radiocarbon, in press, doi:10.1017/RDC.2016.54.
16. Voss H, Kurths J, Schwarz U. (1996) Reconstruction of grand minima of solar activity from $\Delta^{14}C$ data: Linear and nonlinear signal analysis. J. Geophys. Res. 101 (A7): 15,637-15,643.
17. Goslar T (2003) ^{14}C as an Indicator of Solar Variability. in: PAGES News (Past Global Changes) 11(2-3): 12-14.
18. Usoskin IG, Solanki SK, Kovaltsov GA (2007) Grand minima and maxima of solar activity: new observational constraints. A&A 471: 301-309.
19. Poluianov SV, Usoskin IG, Kovaltsov GA (2014) Cosmogenic isotope variability during the Maunder Minimum: Normal 11-year cycles are expected. Solar Phys. 289: 4701-4709.
20. Miyahara H, Masuda K, Muraki Y, Kitagawa H, Nakamura T. (2006) Variation of solar cyclicity during the Spoerer Minimum. J. Geophys. Res. 111: A03103, doi:10.1029/2005JA011016.
21. Miyake F. (2013) Reconstruction of cosmic-ray intensity in the past from measurements of radiocarbon in tree rings. Doctoral thesis, Nagoya University.
22. Nagaya K, et al. (2012) Variation of the Schwabe cycle length during the grand solar minimum in the 4th century BC deduced from radiocarbon content in tree rings. Sol. Phys. 280: 223–236.
23. Steinhilber F, et al. (2012) 9,400 years of cosmic radiation and solar activity from ice cores and tree rings, PNAS 109: 5967-5971.
24. Singarayer JS, et al. (2008) An oceanic origin for the increase of atmospheric radiocarbon during the Younger Dryas, Geophys. Res. Lett. 35: L14707, doi:10.1029/2008GL034074.
25. Usoskin IG, Kromer B (2005) Reconstruction of the ^{14}C production rate from measured relative abundance. Radiocarbon 47: 31-37.
26. Castagnoli G, Lal D (1980) Solar modulation effects in terrestrial production of carbon-14. Radiocarbon 22: 133-158.
27. Kovaltsov GA, Mishev A, Usoskin IG (2012) A new model of cosmogenic production of radiocarbon ^{14}C in the atmosphere. Earth Planet. Sci. Lett. 337: 114–120.
28. Shea MA, Smart DF (1992) Recent and historical solar proton events. Radiocarbon 34: 255-262.
29. Shibayama T, et al. (2013) Superflare on solar-type stars observed with KEPLER. I. Statistical properties of superflares. The Astrophysical Journal Supplement Series 209:5 (13pp), doi:10.1088/0067-0049/209/1/5.

30. Stuiver M, Polach HA (1977) Discussion: reporting of ^{14}C data. Radiocarbon 19: 355–363.
31. Pearson GW, Becker B, Qua F (1993) High-Precision C-14 Measurement of German and Irish Oaks to Show the Natural C-14 Variations from 7890 to 5000 BC. Radiocarbon 35: 93-104.
32. Ramsey CB, et al. (2012) A Complete Terrestrial Radiocarbon Record for 11.2 to 52.8 kyr B.P. Science 338: 370-374.

Acknowledgement

F.M.'s work is supported by JSPS KAKENHI grant number 26887019 and JSPS Program for Advancing Strategic International Networks to Accelerate the Circulation of Talented Researchers under grant number G2602. We also thank the staff of the Arizona AMS Laboratory and ETH AMS Laboratory for their technical assistance. We also thank Dr. H. Tajima and Dr. W. Beck for commenting on our manuscript.

Author Contribution

F.M., T.J. & I.P. designed the measurement and wrote the manuscript. M.S., C.B. & I.P. prepared the wood sample. F.M., T.N., L.W., T.L. & R.C. did the pretreatment of the sample and the AMS measurements. All authors contributed to the discussion.

The authors declare no conflict of interest.

Supporting information

S1. Picture of the tree sample

Figure S1: Image of the bristlecone pine specimen (1971#059) used for our study. This wood was collected in 1971 at Methuselah Walk site (37.3794N, -118.1654W) and archived at Laboratory of Tree-Ring Research, University of Arizona (33).

S2. Comparison with the AD 775 event

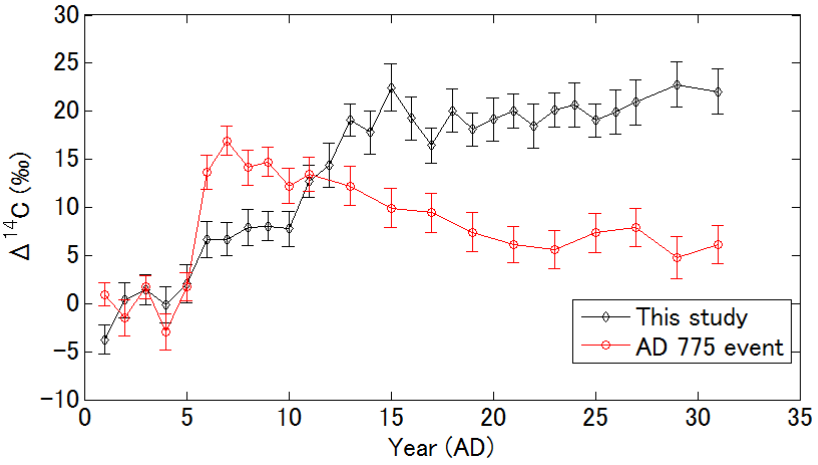

Figure S2: Comparison of ^{14}C measurements between the 5480 BC event (this study) and the AD 775 event[1]. The horizontal and the vertical axis are shifted to compare the two events. We defined the zero points as average values for 5485-5481 BC and AD 770-774.

S3. Annual rapid change in ^{14}C records

There are few examples of an extremely rapid increase rate of ^{14}C except in the two annual cosmic ray events at AD 774-775 and AD 993-994. However, some data in the beginning of the Dalton minimum show also a large increase rate, as can be seem in the annual ^{14}C dataset of Stuiver et al. [1998] (6), i.e. 9.2‰ increase from AD 1796 to AD 1800 and 7.6‰ increase from AD 1808 to AD 1810 (increase rates for these periods are comparable to that of the 5480 BC event). We have also measured this interval using a Japanese cedar sample. However, we did not observe such a rapid increase in the cedar record. Figure S3 shows a comparison of annual ^{14}C datasets (our result, Stuiver et al. [1998] (6), and McCormac et al. [2002] (34)) during the beginning of the Dalton Minimum.

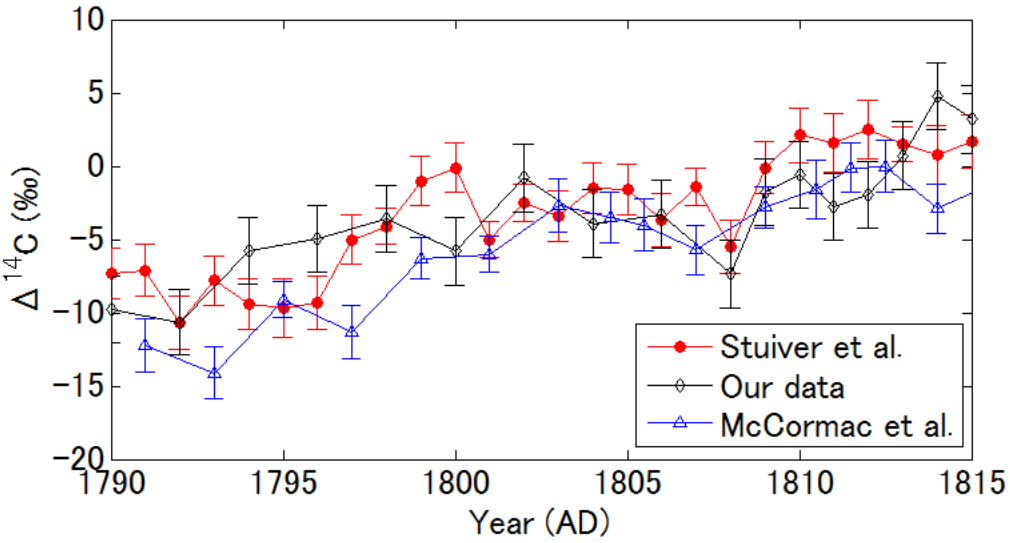

Figure S3: Δ ^{14}C data around the beginning of the Dalton minimum (AD 1790-1815). The circles indicate Stuiver et al. [1998] (North American wood sample) (6), the diamonds indicate our measured result (Japanese wood sample), and triangles indicate McCormac et al. [2002] (Chilean wood sample) (34).

S4. Information of the grand solar minima

Table S1: List of grand solar minima (the Maunder, the Spörer, the Oort, the AD 7th century, and the 4th century BC). The period of grand solar minima are defined according to Usoskin et al. [2007] (18). Increase rates are calculated using first 30 years data of each grand solar minima.

Event	Maunder	Spörer	Oort	AD 7th century	4th century BC
Peirod	AD1640 - AD 1720	AD1390 - AD1550	AD1010 - AD1070	AD650 - AD720	390 BC – 330 BC
Reference	Stuiver et al. [1998] (6)	Miyahara et al. [2006] (20)	Miyake [2013] (21)	Miyake et al. [2013] (35)	Nagaya et al. [2012] (22
Time resolution	1 year	2 years	2 years	2 years	2 years
Increase rate [‰/yr]	0.32	0.18	0.35	0.31	0.42

S5: Production rate and error estimation

We calculated the production rate using the 4-box model which based on Miyake et al. [2012] (2) and Usoskin et al. [2013] (8) (Figure S4), and the 11-box model (10). We assume the start point as a steady state (1.8 [atoms/cm²/sec]), and calculated the ^{14}C input (production rate Q). Figure S5 shows a comparison of the production rate of two box models.

In order to estimate errors of the production rate, we generated 1,000 error series E(t) as:

$E_i(t) = \Delta^{14}C(t) + \Delta^{14}C_{error}(t) \times R_i(t)$

where i=1 to 1,000, $\Delta^{14}C(t)$ is the series of original $\Delta^{14}C$ time series, $\Delta^{14}C_{error}(t)$ is the error series of the original $\Delta^{14}C$ time series, and R(t) is the normal distributed random number series. We converted each $E_i(t)$ series to a production rate series using the 4-box model, and calculated a standard deviation for each age t which is an error of the production rate.

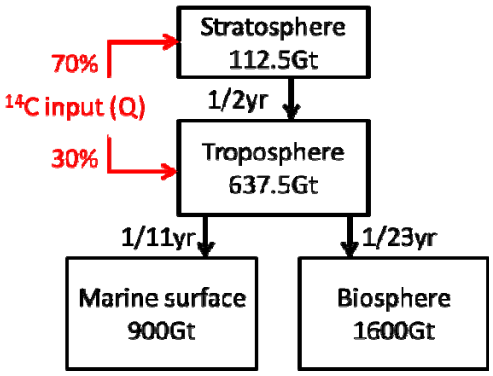

Figure S4: 4-box model of the carbon cycle.

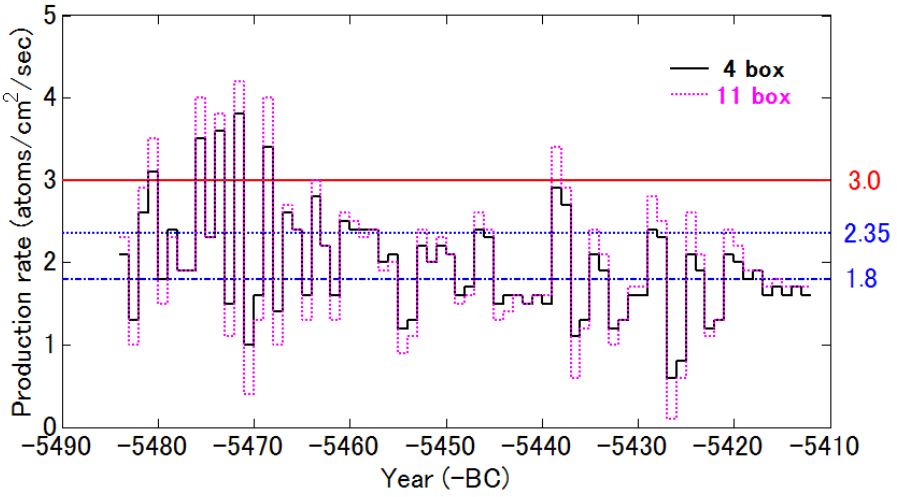

Figure S5: Production rates of the 4-box and the 11-box carbon cycle model.

S6: Comparison with the Maunder Minimum

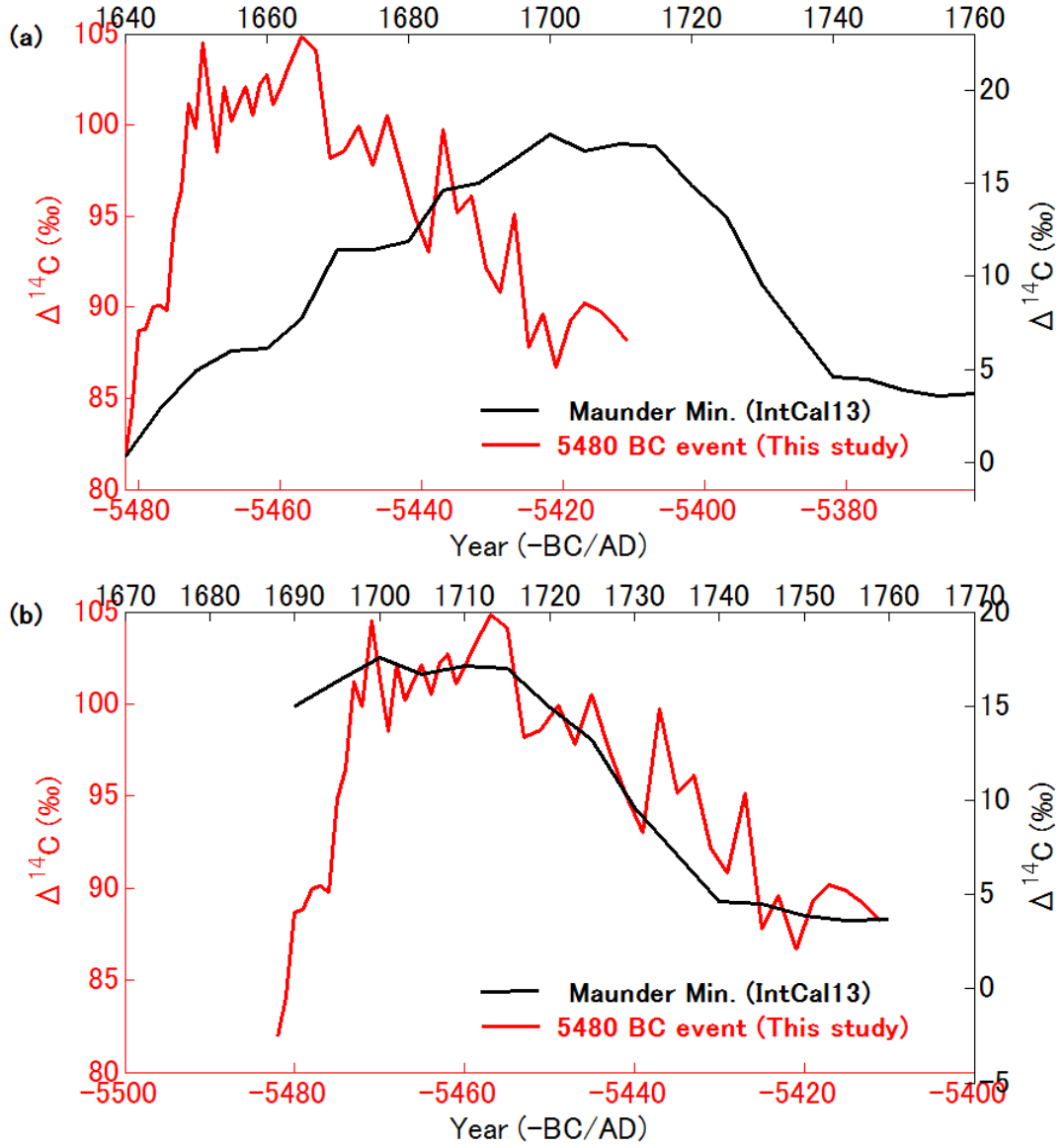

Figure S6: Comparison between the 5480 BC event and the Maunder Minimum (IntCal13 data (1)). (a) Comparison for the period of whole grand solar minimum (AD 1640-1720: the Maunder Minimum, 5482-5411 BC: the present study). Scales of the both axes are same for both series, but the axes were shifted to align the 5482 BC and the AD 1640 data points. (b) Comparison for the attenuated period for the grand solar minima. Scales of the both axes of two series are same. The timescales of the decay of two series are almost same. An approximately decrease timescales are about ~12‰/25yrs.

References of Supporting information

33. Ferguson CW, Graybill DA (1983) Dendrochronology of Bristlecone Pine: A Progress Report. Radiocarbon 25: 287-288.
34. McCormac FG, et al. (2002) Calibration of the radiocarbon time scale for the southern hemisphere: AD 1850-950. Radiocarbon 44: 641-651.
35. Miyake F, Masuda K, Nakamura T (2013) Lengths of Schwabe cycles in the seventh and eighth centuries indicated by precise measurement of carbon-14 content in tree rings. J. Geophys. Res. 118: 8, 7483-7487.